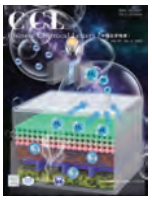
Chinese Chemical Letters 37 (2026) 111788

Contents lists available at ScienceDirect

Chinese Chemical Letters

journal homepage: www.elsevier.com/locate/cclet



Digital microfluidics actuated multiplexed heterogeneous immunoassay with enhanced automation and efficiency

Mengyuan Zhao[a,b,c], Xianming Liu[b,e,*], Haiyue Ye[b,f], Dachuan Ma[b], Yue Hou[b], Hongyu Dong[b], Yangyang Long[b], Ningning Liu[b], Xiaoxu Wang[d], Xiaodan Yu[d], Yahong Chen[a,c,**], Xinmiao Liang[b,e,*], Yao Lu[b,e,*]

[a] College of Chemistry and Green Catalysis Center, Zhengzhou University, Zhengzhou 450001, China
[b] Key Laboratory of Phytochemistry and Natural Medicines, Dalian Institute of Chemical Physics, Chinese Academy of Sciences, Dalian 116024, China
[c] College of Chemistry & Chemical Engineering, Zhoukou Normal University, Zhoukou 466001, China
[d] Affiliated Center Hospital, Dalian University of Technology, Dalian 116024, China
[e] University of Chinese Academy of Sciences, Beijing 100049, China
[f] Southen University of Technology, Shenzhen 518000, China

ARTICLE INFO

Article history:
Received 28 November 2024
Revised 11 June 2025
Accepted 4 September 2025
Available online 5 September 2025

Keywords:
Digital microfluidics
Mulitpled immunoassay
Automation
Multiplexed
FluoroPel

ABSTRACT

Digital microfluidics (DMF) shows great promise in addressing the need for miniaturization and automation in immunoassay detection. Despite recent advances, an automatically operated, multiplexed heterogeneous immunoassay platform powered by DMF remains underdeveloped. Here we present a DMF platform for automated and multiplexed heterogeneous immunoassay detection by coupling spatial barcoding with automatic and uniform droplet dispensing. FluoroPel was selected as a robust hydrophobic reagent for coating the DMF top plate, and it also served as the substrate for the immuno-reaction. Its mechanical robustness was further enhanced with a Cytop CTL-809A adhesive layer under the top hydrophobic layer. Hourglass-shaped electrode patterns ensured consistent and uniform distribution of immunoassay reagents, with volume variation down to 1.0 %. The analysis duration was significantly reduced from 75 min to 20 min after a heating module was integrated to elevate the immuno-reaction temperature to 37 °C. Utilizing a compact instrument featuring a multi-droplet manipulation protocol, we successfully implemented fully operated, multi-sample, multiplexed immunoassays using recombinant proteins on cell culture supernatants on the DMF platform. This innovative platform significantly enhances the efficiency, reliability, and degree of automation of DMF-actuated multiplexed heterogeneous immunoassays, potentially providing a viable solution for field deployment and multi-sample parallel diagnosis.

© 2026 Published by Elsevier B.V. on behalf of Chinese Chemical Society and Institute of Materia Medica, Chinese Academy of Medical Sciences.

In life sciences, advances in discovering new molecular biomarkers deepen our understanding of physiological processes, driving the need for innovating immunoassay methods [1]. Despite this, enzyme-linked immunosorbent assay (ELISA) [2] is a widely used tool for identifying physiological regulators, such as cytokines, which work synergistically with other proteins in immune extracellular and intracellular responses [3,4]. However, conventional immunoassay detection requires large amounts of expensive antibodies, high labor costs, and cumbersome instruments, while microfluidics-based POCT platforms meet the core needs for automation, multiplexing, and rapid detection, highlighting the growing demand for miniaturization and automation in immunoassays [5–7]. Digital microfluidic (DMF) chips, which maneuver liquid droplets as microcarriers of samples based on electrowetting on dielectrics (EWOD) [8,9], would be appealing to conduct heterogeneous biosensing with low sample consumption [10]. Typically, on a DMF device, discrete droplets in micro- or sub-microliters [11] can be actuated under EWOD force by tuning the wettability of the chip surface with electric potentials. Equally important, controlled by switches on electrodes, the functional manipulation of droplets [12], which includes transportation, dispensing, merging, and splitting, is highly programmable [13,14] and attractive for automation in the manipulation of miniaturized liquid samples.

* Corresponding author at: Key Laboratory of Phytochemistry and Natural Medicines, Dalian Institute of Chemical Physics, Chinese Academy of Sciences, Dalian 116024, China.
** Corresponding author at: College of Chemistry and Green Catalysis Center, Zhengzhou University, Zhengzhou 450001, China.
E-mail addresses: liuxianming@dicp.ac.cn (X. Liu), chenyahong@zknu.edu.cn (Y. Chen), liangxm@dicp.ac.cn (X. Liang), luyao@dicp.ac.cn (Y. Lu).

https://doi.org/10.1016/j.cclet.2025.111788
1001-8417/© 2026 Published by Elsevier B.V. on behalf of Chinese Chemical Society and Institute of Materia Medica, Chinese Academy of Medical Sciences.

Various heterogeneous immunoassays, such as fluorescence [15], chemiluminescence [16], and electrochemiluminescence [17], have been demonstrated on the DMF platform. Wheeler's group [18] developed a portable DMF-engaged ELISA platform for on-site measles and rubella immunoglobulin G testing. Another study [19] utilized magnetic beads to replace microplates as the solid phase, transitioning the immunoreaction from two-dimensional to three-dimensional and further enhancing the sensitivity of the immunoassay. In Chen's work [20] functionalized magnetic beads and gold nanoparticle labels were used to construct a magnetically controlled immunosensing probe, developing an advanced immuno-HCR assay with a pH meter readout. However, for bead-supported detection [21–23], specificity and ease of sample handling have to be leveraged. The planar substrate-supported detection strategy may free the need for embedding any external gears for the manipulation of magnetic microbeads. For example, Wheeler's group [24] introduced a straightforward method that DMF chip surface was used for antibody immobilization. We previously developed spatial barcoding-enabled highly multiplexed immunoassay with digital microfluidics [25]. However, this study has not yet incorporated crucial functionalities such as programmed droplet dispensing, which DMF chips excel in The process still necessitates many manual operations of liquids, unfortunately leading to an insufficient degree of automation for driving high-protein reagents and resulting in prolonged immuno-reaction times.

In this study, we realized the automation of multi-sample, multiplexed immunoassay detection on an innovatively designed digital microfluidic platform by incorporating spatial barcoding and programmed droplet manipulation. Using carboxylic group end-functionalized Cytop as an extra adhesion layer, FluoroPel film was applied to the DMF top plate and bound firmly with the Indium Tin Oxide (ITO) upper plate as the immuno-reaction substrate on which spatial barcodes of capture antibodies was later formed for heterogeneous immunoassay detection (Fig. 1A). An hourglass-shaped electrode design was adopted [26,27], eliminating the need to introduce an additional external module such as volume feedback [23,28] but still enabling reliable dispensing of droplets that sequentially carried samples of interests and reagents for heterogeneous ELISA reactions. A close-looped heater was integrated to accurately elevate the reaction temperature and accelerate the immuno-reaction to be completed within 20 min. Eventually, we successfully realized automated, multi-sample, parallel immuno-reactions on the DMF platform using a tailor-designed compact instrument automated with a multi-droplet manipulation protocol.

Details regarding the materials, DMF chip fabrication, system assembly, and operational procedures are provided in the first sec-

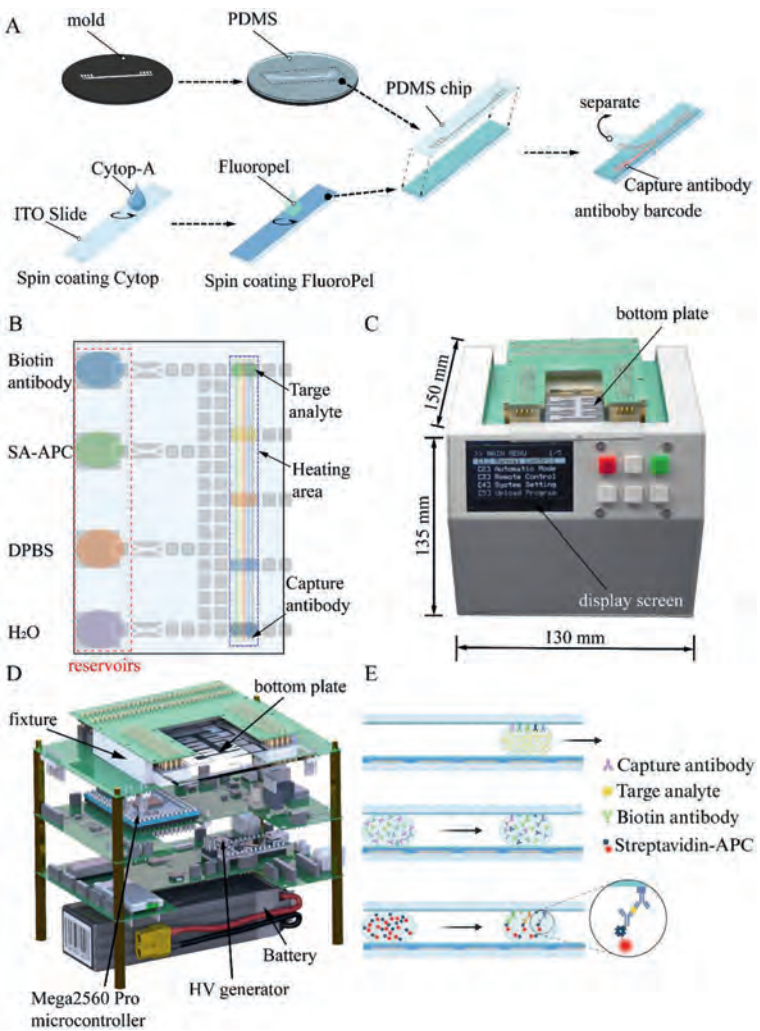


Fig. 1. The compact DMF instrument for automating immunoassay operations. (A) The workflow of the antibody barcode immobilization. (B) The schematic illustration of how droplets are allocated on the device (top view). (C) A photograph of our compact-sized DMF device. (D) A rendered schematic showing the internal layout inside the DMF platform. (E) The schematic shows the sequential delivery of sample and reagent droplets through the immuno-reaction zones.

tion of Supporting information. Briefly, to overcome the labor-intensive manual separation steps inherent in heterogeneous immunoassays, a digital microfluidic (DMF) device was fabricated and assembled. The DMF chip typically consisted of a bottom plate and a top functional plate. The bottom plate accommodates driving electrodes which can be activated electrically. Besides functioning as the ground electrode to form an electric loop with the droplets, driving electrodes, switches, and the power source, the top plate also serves as the substrate for heterogeneous immunoassay. To enable multiplexed detection, a PDMS microchip was fabricated with and attached to the top plate, forming parallel microchannels. The capture antibodies of cytokines, including IL-1β, IL-6, IL-8, TNF-α, and MCP-1, approximately 2 μL each, were introduced into these channels and incubated for 1 h. After incubation, the remaining capture antibodies were evacuated from the channels using the vacuum pump. After the PDMS chip was carefully peeled from the tip plate, the assembly of the DMF device was achieved by aligning the top and bottom plates with a spacer of 0.125 mm-thick polyimide film placed in between. The allocation of sample/reagents in droplets engaged with DMF-engaged actuation is illustrated in Fig. 1B.

To automate liquid handling, a compact-sized DMF platform was custom-made (Fig. 1C), with a small footprint of 150 × 135 × 120 mm (length × width × height) and a weight of only 1.3 kg. The control system consists of the DMF chip fixture, three printed circuit boards (PCB) circuitries, as well as a rechargeable battery (Fig. 1D). The control system and the peripheral modules were powered by a rechargeable 12 V battery, potentially enabling on-site and portable use. The DMF instrument could automatically realize the sequential delivery of the sample and reagents through the immuno-reaction zones, as depicted in Fig. 1E.

We evaluated three commonly used hydrophobic materials in digital microfluidics to select the appropriate substrate suitable for a robust DMF-based immunoassay. The results showed that the hydrophobic film formed by FluoroPel 1101 V exhibited a contact angle of 123.7° (Figs. 2A and B), superior to those of the Teflon-coated surfaces. Notably, FluoroPel 1101 V also showed superiority in actuating protein-containing liquid that could realize actuation of up to 50 % fetal bovine serum solution, demonstrating that FluoroPel 1101 V would be a suitable candidate substrate for DMF-based immunoassay. We then evaluated the protein binding performance of the FluoroPel 1101 V material using FITC-BSA as the coating protein. The fluorescence distribution across the slide (Fig. 2C) showed that the attachment of proteins on the FluoroPel surface is strong and evenly distributed (fluorescence coefficient of variation = 4.8 %, n = 4000) (Fig. 2D). The AFM characterizations showed that the roughness of the surface increased from 0.664 nm to 2.66–4.339 nm (Table S1 in Supporting information) and the surface peak-to-valley value increased from 4.3 nm (Fig. 2Ea) to 14.9–22.9 nm (Figs. 2Eb and c and Fig. S1 in Supporting information), after antibody coating respectively. These results demonstrated that FluoroPel 1101 V could be an ideal substrate to for immobilizing capture antibodies in the DMF platform.

Previously, a Teflon-coated ITO glass slide was used as a substrate for immuno-reaction, but the Teflon layer often detached due to weak bonding under shear forces during removal [25,28]. To address this, Cytop CTL-809A, containing carboxylic groups, was applied as an adhesive layer between the hydrophobic film and the ITO substrate, significantly improving bonding strength. Tests showed the FluoroPel layer with Cytop had a hardness of 2B compared to 6B without it (Fig. 2F), demonstrating enhanced robustness for use in immuno-reactions. The above results demonstrate that the FluoroPel 1101V-coated ITO glass slide could be used as the substrate for immuno-reaction with excellent robustness which is boosted by the Cytop-COOH adhesive layer.

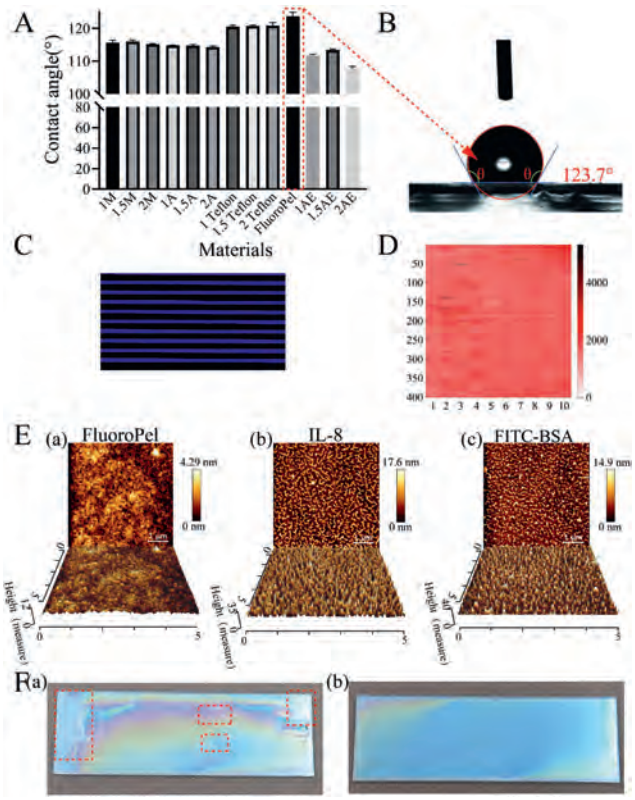


Fig. 2. Characterizations of DMF Top Plates. (A) Contact angle measurements of DI water on various hydrophobic surfaces. (B) Fluoropel-coated surface contact angle image. (C) Fluorescence image of FITC-BSA on the modified ITO surface under 488 nm excitation. (D) Heat map of fluorescence intensity across 400 randomly selected 10 × 10 μm regions. (E) 5 × 5 μm AFM 2D and 3D surface mapping of different antibody adsorbed on a hydrophobic surface (a) without antibody, (b) IL-8, (c) FITC-BSA. (F) (a) Hydrophobic layer damage (red boxes) without an adhesive layer, (b) intact hydrophobic layer with adhesive layer.

To optimize reagent and sample dispensing on DMF chips during immuno-reaction, we redesigned the dispensing electrodes, combining arc-shaped outer electrodes with a central hourglass pair (Fig. 3A). This design improved droplet generation reliability. By sequentially activating electrodes, droplets were extruded and separated efficiently with reduced cut-off pressure due to optimized geometric patterns (Fig. 3B). Four necking electrode radii (1.0–2.5 mm) and various liquid storage electrode sizes were tested (Fig. S2 in Supporting information). Using vision analysis (Fig. S3 in Supporting information), we found that a 2.0 mm neck radius and a 5.0 × 6.0 mm storage electrode produced droplets with the lowest CV (1.0 %) and highest volume consistency, making this configuration ideal for subsequent immunoassay applications (Fig. 3C).

To increase analysis efficiency, three strategies were employed to speed up molecular diffusions inside droplets and their interaction with the antibody barcodes to shorten the turnaround time, including active mixing (moving reagents back and forth on electrodes), pre-mixing (combining primary and secondary antibodies before reactions), and heating (maintaining reaction zones at 37 °C), as depicted in Fig. 4A. The active mixing strategy would increase the risk of biological contamination which reduces the operational longevity of the chip. Another drawback is that the fluorescent signals were significantly lower, (Fig. 4Ba). The pre-mixing approach demonstrates significantly lower sensitivity on some of the analytes (Fig. 4Bb). Heating shortened reaction time from 75 min to under 20 min with comparable or stronger detection signals, making it the preferred approach (Fig. 4Bc).

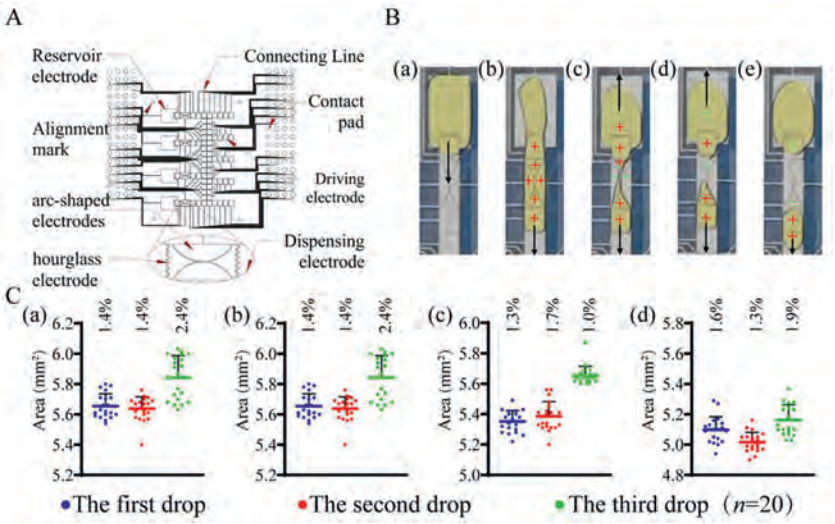


Fig. 3. Optimization of the dispensing electrodes on the DMF bottom plate. (A) The design of electrodes pattern the DMF bottom plate. (B) Captured images showing the dispensing process of the dispensing electrode. The arrow indicates the moving direction of the droplets while "+" and "-" represent the activated and deactivated electrodes, respectively. (C) Uniformity statistics including the coefficient variation, of dispensed droplets with projected area under different combinations of electrode sizes for comparison. (a-d) The sizes of the liquid separation electrode are 1.0, 1.5, 2.0, and 2.5 mm, respectively.

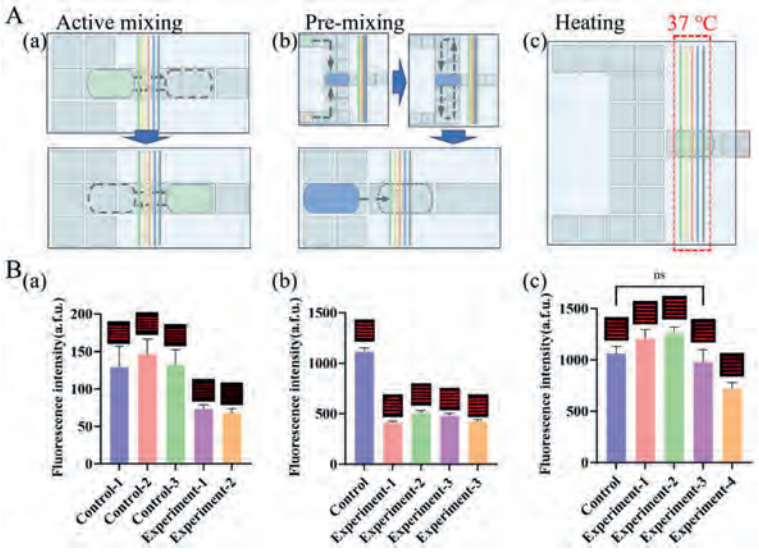


Fig. 4. Comparison of different strategies to escalate the analysis efficiency for DMF-actuated immunoassay. Schematic diagram (A) and fluorescence readouts (B) of (a) active mixing, (b) pre-mixing and (c) heating.

We further validated the feasibility of the DMF platform for multiplexed heterogeneous immunoassay detection with different recombinant proteins, including IL-1β, IL-6, TNF-α, MCP-1, and IL-8, which play crucial roles as important immune and oncogenic functional markers and regulators (Fig. 5A). We used air as the surrounding medium for the droplets instead of carrier fluids such as silicone oil. A typical process of DMF-automated multiplexed heterogeneous immuno-reaction was demonstrated in Fig. S4 (Supporting information). The standard titration curves were successfully obtained with fluorescence readouts in a four-parameter logistical regression model (4PL) (Fig. 5B), with the highest fitting coefficient of 99.3 %. The limit of detection (LOD) varies, depending on the affinity within antigen-antibody pairs. To demonstrate the applicability of DMF-automated immunoassay for biology studies, we applied this platform with different cell supernatants, including cholangiocarcinoma cells (HUCCT1), umbilical vein endothelial cells (HUVEC), cardiomyocytes (AC16), and lymphoma cells (U937), with the 10 % FBS-supplemented cell culture medium as the control group (0.2 % Tetronic 90R4). Fig. 5C shows the fluorescence image of 5-plexed protein detection from collected supernatants. Fig. 5D presents the fluorescence intensities of five cytokines across four different cell types, along with a control. The fluorescence intensity, measured in arbitrary units (a.f.u.), indicates the expression levels of each cytokine within these cells. For example, U937 cells show the highest overall cytokine expression, indicating a robust immune response profile. In contrast, HUVEC cells show lower overall cytokine levels, which might indicate their endothelial origin and different functional roles from immune cells like U937. AC16 and HUCCT1 cells show higher levels of MCP-1 secretion, which might indicate an ongoing inflammatory response within the tumor, contributing to cancer progression.

In conclusion, this study successfully demonstrates a high level of automation in multi-sample, multiplexed immunoassay detection on a digital microfluidic platform. Fabricating double-layered hydrophobic films and optimizing electrode patterns led to a robust barcode of capture antibodies and consistent liquid distribu-

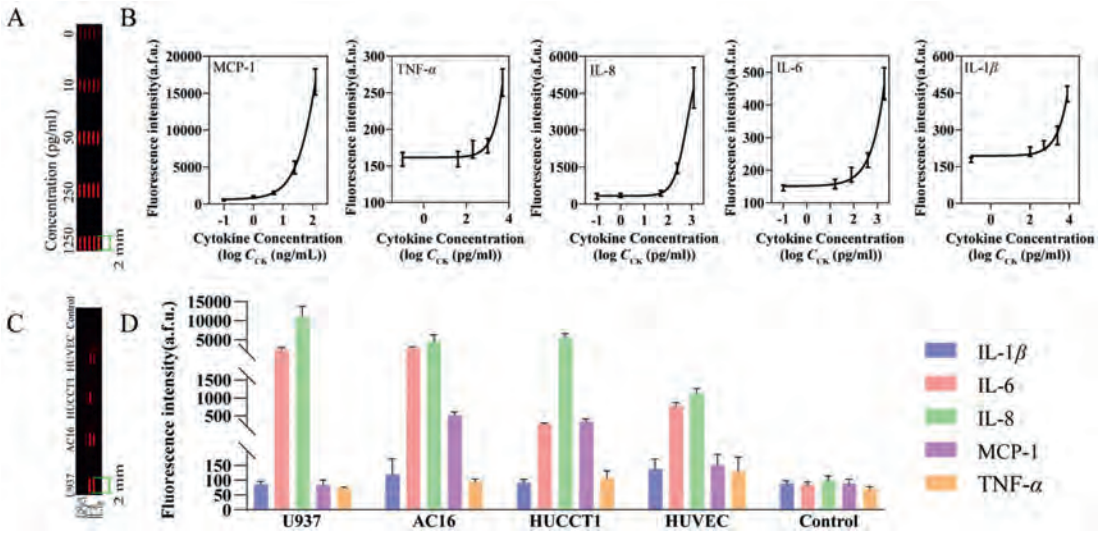


Fig. 5. Multiplexed immunoassay detection on the DMF platform. (A) IL-8 detection with varying concentrations on the ITO top plate. (B) The immunoassay titration curve of concentration gradient dilution fits with the four-parameter logistic (4PL) curves. (C) Fluorescence detection of the ITO top plate for different cell supernatant immunoassay results. (D) Multiplexed immunoassay fluorescence intensity chart of four cell supernatants, with U937, AC16, HUCCT1, HUVEC, and the control group shown, respectively.

tions for immuno-reaction completion. To enhance the efficiency of DMF-actuated immunoassays, three strategies were explored: active mixing, pre-mixing, and heating. The first two approaches either increased the risk of cross-contamination or resulted in reduced sensitivity. In contrast, elevating the immuno-reaction temperature to 37 °C significantly improved reaction efficiency, enabling the completion of the immunoassay within 20 min. The compact, battery-powered instrument, equipped with a multi-droplet control protocol, achieves efficient and reliable immunoassays. Compared with other DMF-actuated heterogenous immunoassay detection, the work developed showed superiority summarized in Table S2 (Supporting information), including detection time, dependence on magnetic beads, degree of automation, number of indicators measured, and number of samples tested. It is worth noting that the detection capacity of the platform can be further improved by increasing the number of parallel stripes, by which capture antibodies are spatially defined, for higher detection multiplexity. These advancements offer a significant possibility for field deployment and multi-sample parallel diagnostics, marking a substantial improvement in the performance and applicability of DMF-actuated heterogeneous multiplexed immunoassays.

Declaration of competing interest

The authors declare that they have no known competing financial interests or personal relationships that could have appeared to influence the work reported in this paper.

CRediT authorship contribution statement

Mengyuan Zhao: Writing – review & editing, Writing – original draft, Methodology, Investigation, Formal analysis, Data curation. **Xianming Liu:** Writing – review & editing, Writing – original draft, Supervision, Investigation, Funding acquisition, Formal analysis, Data curation, Conceptualization. **Haiyue Ye:** Investigation, Data curation. **Dachuan Ma:** Investigation, Data curation. **Yue Hou:** Software, Investigation. **Hongyu Dong:** Software, Investigation. **Yangyang Long:** Software, Formal analysis. **Ningning Liu:** Data curation. **Xiaoxu Wang:** Resources, Investigation, Data curation. **Xiaodan Yu:** Resources, Investigation. **Yahong Chen:** Supervision, Resources, Project administration, Conceptualization. **Xinmiao Liang:** Supervision, Project administration, Funding acquisition, Conceptualization. **Yao Lu:** Writing – review & editing, Writing – original draft, Supervision, Resources, Project administration, Funding acquisition, Conceptualization.

Acknowledgments

This work was supported by the National Key R&D Plan of China (No. 2023YFB3210400), the National Natural Science Foundation of China (Nos. 31927802, 22574155), Liaoning Provincial Natural Science Foundation Young Scientists Fund Project (Category A, No. 2025JH6/101100013) and the fund from the Dalian Institute of Chemical Physics (Nos. DICP I202451, DMU-2&DICP UN202503), and the Postgraduate Education Reform and Quality Improvement Project of Henan Province (No. YJS2023JD37). The authors would like to thank Mr. Yong Zhang from AGC Inc. for Cytop reagents and valuable discussions.

Supplementary materials

Supplementary material associated with this article can be found, in the online version, at doi:10.1016/j.cclet.2025.111788.

References

[1] G. Xing, Y. Shang, X. Wang, et al., Chin. Chem. Lett. 35 (2024) 109491.
[2] D.H. Wu, Q.L. Zhao, J. Sun, et al., Chin. Chem. Lett. 34 (2023) 107672.
[3] C. Liu, D. Chu, K. Kalantar-Zadeh, et al., Adv. Sci. 8 (2021) 2004433.
[4] E.A. van Aalen, B.J.H.M. Rosier, T. Jansen, et al., Anal. Chem. 95 (2023) 8922–8931.
[5] C. Li, W. Zhou, A.G. Ruiz, et al., Trac-Trends Anal. Chem. 177 (2024) 117809.
[6] T. Colasanti, F. Conti, Methods Mol. Biol. 2750 (2024) 135–141.
[7] H. Yun, H.J. Jeong, Spectrochim. Acta. A Mol. Biomol. Spectrosc. 310 (2024) 123973 -123973.
[8] B. Bruno, C. R. Acad. Sci. Ser. II 317 (1993) 157–163.
[9] X. Rui, S. Song, W. Wang, et al., Biomicrofluidics 14 (2020) 061503.
[10] C. Yang, X. Gan, Y. Zeng, et al., Biosens. Bioelectron. 242 (2023) 115723.
[11] X. Xu, L. Lin, J. Yang, et al., Nano Today 46 (2022) 101596.
[12] X.M. Liu, D.C. Ma, H.Y. Ye, et al., Trac-Trends Anal. Chem. 166 (2023) 117153.
[13] S.K. Cho, H.J. Moon, C.J. Kim, J. Microelectromech. Syst. 12 (2003) 70–80.
[14] Y. Fouillet, J.L. Achard, C. R. Phys. 5 (2004) 577–588.
[15] M.J. Jebrail, H. Yang, J.M. Mudrik, et al., Lab Chip 11 (2011) 3218–3224.
[16] B. Yang, L. Shi, Q.R. Tang, et al., Lab Chip 23 (2023) 785–792.
[17] M.H. Shamsi, K. Choi, A.H.C. Ng, et al., Biosens. Bioelectron. 77 (2016) 845–852.
[18] A.H.C. Ng, R. Fobel, C. Fobel, et al., Sci. Transl. Med. 10 (2018) 12.
[19] S. He, Q. Huang, Y. Zhang, et al., Chin. Chem. Lett. 32 (2021) 1462–1465.

[20] J.C. Chen, H.F. Xue, Q.Y. Chen, et al., Chin. Chem. Lett. 30 (2019) 1631–1634.
[21] T.C. Tsai, Y.W. Wang, M.S. Lee, et al., Int. J. Mol. Sci. 25 (2024) 4006.
[22] W. Hsu, Y.T. Shih, M.S. Lee, et al., Biosens. Basel. 12 (2022) 340.
[23] M.S. Lee, Y.C. Chang, H.Y. Huang, et al., J. Pharm. Biomed. Anal. 219 (2022) 114877.
[24] E.M. Miller, A.H. Ng, U. Uddayasankar, et al., Anal. Bioanal. Chem. 399 (2011) 337–345.
[25] H. Li, X. Liu, F. Zhu, et al., Biosens. Bioelectron. 215 (2022) 114557.
[26] H. Wang, L. Chen, Nanot. Rev. 10 (2021) 857–869.
[27] W. Wang, Micromachines 13 (2022) 484.
[28] L. Lu, H. Zhang, Y. Wang, et al., ACS Appl. Mater. Interfaces 15 (2023) 6526–6535.